Available online at www.sciencedirect.com

SciVerse ScienceDirect

Ceramics International 39 (2013) 3205–3210

CERAMICS INTERNATIONAL

www.elsevier.com/locate/ceramint

Dielectric and ferroelectric study of KNN modified NBT ceramics synthesized by microwave processing technique

Sridevi Swain[a], Pawan Kumar[a,*], Dinesh K. Agrawal[b], Sonia[c]

[a]Department of Physics, National Institute of Technology, Rourkela 769008, India
[b]Materials Research Institute, Pennsylvania State University, University Park, PA 16802, USA
[c]Department of Chemistry, National Institute of Technology, Rourkela 769008, India

Received 24 September 2012; received in revised form 2 October 2012; accepted 2 October 2012
Available online 9 October 2012

Abstract

Morphotropic phase boundary (MPB) composition, $0.93Na_{0.5}Bi_{0.5}TiO_3$–$0.07K_{0.5}Na_{0.5}NbO_3$/NBT–KNN was synthesized by microwave heating. The optimized calcination conditions for single perovskite phase formation were 800 °C for 40 min, whereas the sintering was carried out at 1150 °C for 20, 30 and 40 min. The MPB composition, sintered for 30 min, showed better properties: nearly uniform and larger grain size of ~2.52 μm, room temperature (RT) dielectric constant (ε_r) ~1180 at 1 kHz, a relatively high bulk density (ρ) ~5.49 g/cc, remnant polarization ($2P_r$) ~3.3μC/cm^2 and coercive field (E_c) ~5.8 kV/cm. Diffuse phase transition was observed for all the ceramics with highest diffusivity factor, γ~1.65 in MPB composition sintered for 30 min.

Keywords: Lead free ferroelectrics; Microwave heating; Morphotropic phase boundary; Perovskite phase

1. Introduction

Ferroelectric ceramics are known for their widespread applications like in capacitors, piezoelectric actuators, sensors and transducers, non-volatile random access memory (NvRAM) etc. Lead based ferroelectric ceramics such as lead titanate ($PbTiO_3$) and its solid solution with $ZrTiO_3$ at morphotropic phase boundary (MPB) exhibit excellent ferroelectric and piezoelectric properties [1]. However, the high toxicity of lead oxide has caused serious environmental problems. Therefore, recently extensive investigations have been carried out to develop lead-free systems with potentially comparable ferroelectric properties [2]. Lead free ferroelectric materials with perovskite structure have attracted much attention since they are easy to prepare and the structure is simple compared to other structures [3]. Barium titanate (BT), sodium bismuth titanate (NBT), potassium niobate (KN), potassium sodium niobate (KNN) and potassium tantalate niobate (KTN) with perovskite structure are some of the promising lead free ferroelectric systems [4]. In 1960, Smolenskii et al. [5] first discovered $Na_{0.5}Bi_{0.5}TiO_3$ (NBT) system. Because of excellent ferroelectric properties and a high Curie temperature (T_C= 320 °C), NBT was considered as a promising lead free system. However, pure NBT ceramics show high coercive field (E_C=73 kV/cm), and difficulties in polarization switching [6]. In order to overcome these problems many substitutions at A- and B-sites in NBT system have been investigated by many researchers [7–9]. Solid solutions of NBT with BT, KNN, and BKT etc. have also been prepared. Among these different solid solutions, NBT–KNN is considered to be a potential system for replacing lead based counterparts [10–12]. In this system MPB is found at $0.93Na_{0.5}Bi_{0.5}TiO_3$–$0.07K_{0.5}Na_{0.5}NbO_3$ composition as reported by Kounga et al. [13]. In this work, MPB composition of the NBT–KNN system is synthesized by the microwave heating technique. The structural, microstructure, and electrical properties of the NBT–KNN system have been investigated and discussed in detail.

*Corresponding author. Tel.: +91 661 2462726.
E-mail addresses: pvn77@rediffmail.com, pawankumar@nitrkl.ac.in (P. Kumar).

0272-8842/$ - see front matter © 2012 Elsevier Ltd and Techna Group S.r.l. All rights reserved.
http://dx.doi.org/10.1016/j.ceramint.2012.10.005

2. Experimental procedure

MPB composition, $0.93Na_{0.5}Bi_{0.5}TiO_3$–$0.07K_{0.5}Na_{0.5}NbO_3$ was synthesized by the microwave processing technique. Na_2CO_3(Merck), Bi_2O_3 (Loba Chemie), TiO_2 (Merck), K_2CO_3(Loba Chemie) Nb_2O_5 (Merck) (of purity ≥ 99%) with stoichiometric proportions were used as raw materials. The starting powders were ball milled using zirconium balls and using acetone as the grinding medium. 800 °C for 40 minutes processing step was optimized as the calcination condition for single perovskite phase formation. Single perovskite phase formation was confirmed by the X-ray diffraction (XRD) technique. The calcined powders were mixed with 2 wt% polyvinyl alcohol (PVA) and uniaxially pressed under ~60 MPa pressure using hydraulic press into disks of diameter ~10 mm and thickness ~1 mm. The microwave sintering of the sample was carried out at 1150 °C for 20, 30 and 40 min with a heating rate of 30 °C/min by placing the pellets at the center of a 4.4 kW, 2.45-GHz multimode microwave cavity. The microwave furnace temperature was recorded by using a Raytek non-contact sensor (XRTG5). The density of ceramic samples was measured by the Archimedes principle using the kerosene medium. The sintered microstructures were observed using a JEOL T-330 scanning electron microscope (SEM). Silver paste was applied on both sides of the samples for the electrical measurements. Dielectric constant (ε_r) was measured as a function of temperature at different frequencies; whereas, room temperature ε_r, and dielectric loss (tan δ) were measured with varied frequencies using a computer interfaced HIOKI 3532-50 LCR-HITESTER. A conventional Sawyer–Tower circuit was used to measure the polarization vs. electric field (*P*–*E*) hysteresis loops [14].

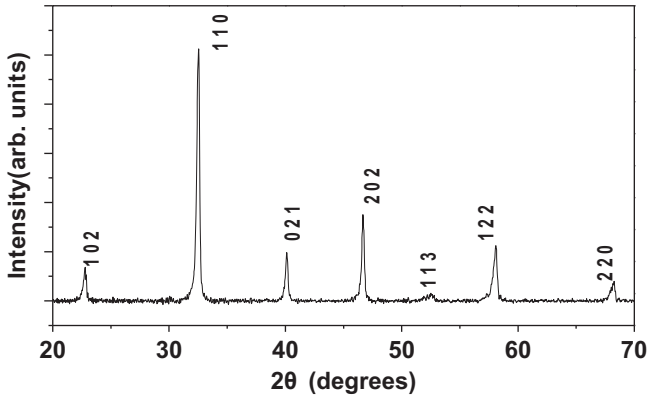

Fig. 1. XRD pattern of NBT–KNN ceramics calcined (MW) at 800 °C for 40 min.

3. Results and Discussion

Fig. 1 shows the XRD pattern of NBT–KNN ceramics calcined at 800 °C for 40 min. The diffraction pattern reveals the development of single perovskite phase without any trace of secondary phase. All peaks are accounted for perovskite phase only. It is reported that pure NBT ceramics possess rhombohedral structure [15] and with the solid solution of KNN system there exists a MPB region as reported by Kounga et al. The peaks were indexed by using the standard computer program package

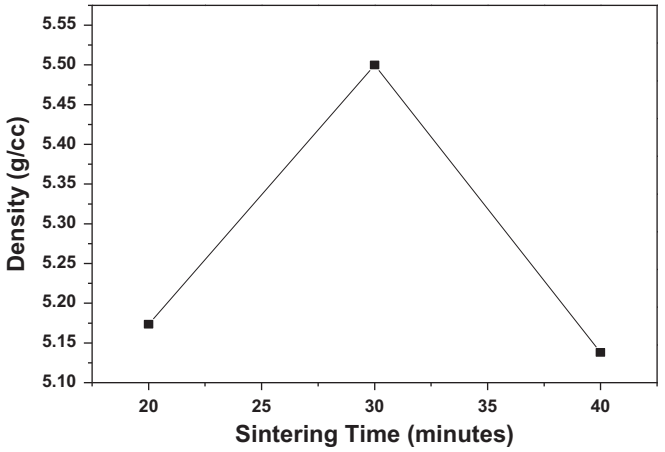

Fig. 2. Variation of density with sintering time of MW processed NBT–KNN ceramics.

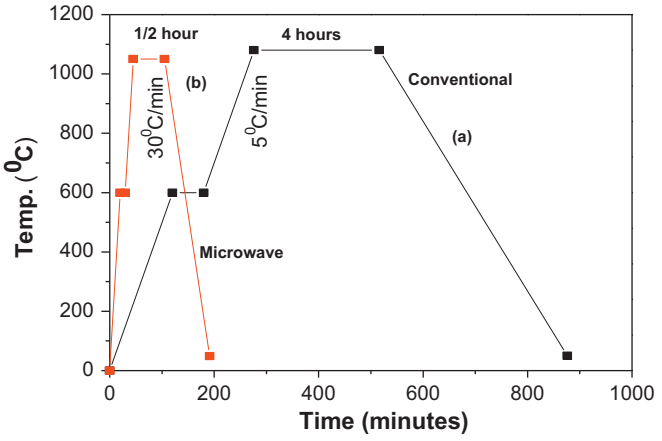

Fig. 3. Time vs. temperature sintering profile of conventional and microwave sintered NBT–KNN samples.

Table 1
Structural and electrical parameters of microwave processed NBT–KNN ferroelectric ceramics.

Microwave sintering time (min)	Density (g/cc)	porosity	Average grain size (μm)	T_m (°C)	ε_r at RT and at 1 kHz	T_d (°C)	$\varepsilon_{r\ max}$ at T_m and at 1 kHz	RT tan δ at 1 kHz	Diffusivity factor (γ)
20	5.17	0.012	1.24	177	1036	97	2349	0.044	1.55
30s	5.49	0.062	2.52	181	1180	104	2661	0.041	1.65
40	5.13	0.090	1.66	183	1056	115	2463	0.039	1.21

'Powdmult' [16]. In the present study, the NBT–KNN ceramics show rhombohedral and pseudo cubic phase, this confirms the MPB nature of this composition.

The experimental density (ρ_{ex}) of the sintered NBT–KNN ceramics was measured by the Archimedes principle and given in Table 1 and plotted in Fig. 2. The initial increase of ρ_{ex} with the increase of sintering time may be due to the formation of liquid phase across the grain boundary [17]. It is known that the formation of liquid phase is critical for densification of NBT–KNN based ceramics which leads to rearrangement of particles providing more effective packing. Maximum ρ_{ex} is obtained in case of NBT–KNN ceramics sintered at 30 min. The densities calculated to be higher than the conventional processed NBT–KNN ceramics [22]. The advantages of microwave processing over conventional processing are manifold: substantial reduction of sintering conditions, less energy consumption, better properties, fine microstructure, etc. This is due to the fact that the way microwave interacts with the material providing rapid, selective, volumetric and uniform heating [18]. Time vs. temperature profile of microwave and conventionally sintered NBT–KNN is shown in Fig. 3 [19]. Fig. 4 shows the SEM micrographs of NBT–KNN ceramics sintered at 1150 °C for 20, 30, and 40 min. SEM micrographs show the non-uniform arrangement of grains. The non-uniformity of grains may be attributed to substitution of KNN in the NBT system. Non-uniform microstructure is the characteristic of the KNN system [20]. The average grain size is calculated by the linear intercept method and shown in Table 1.

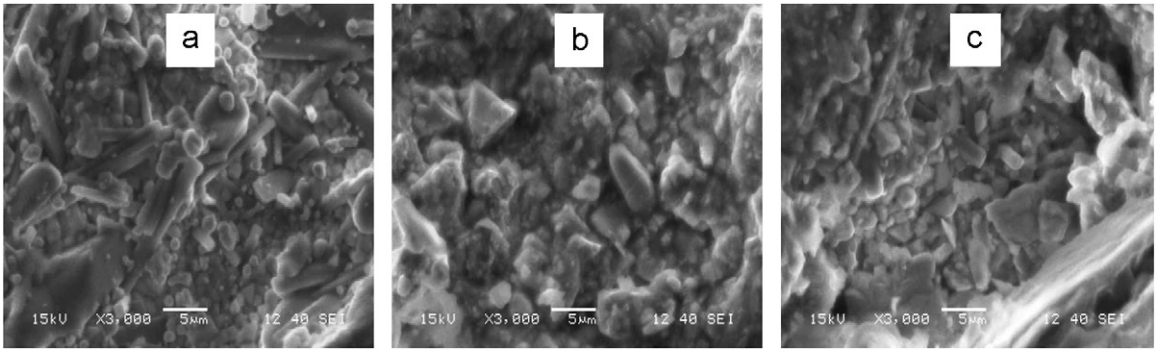

Fig. 4. SEM micrographs of NBT–KNN ceramics sintered in MW furnace at 1150 °C for (a) 20, (b) 30 and (c) 40 min.

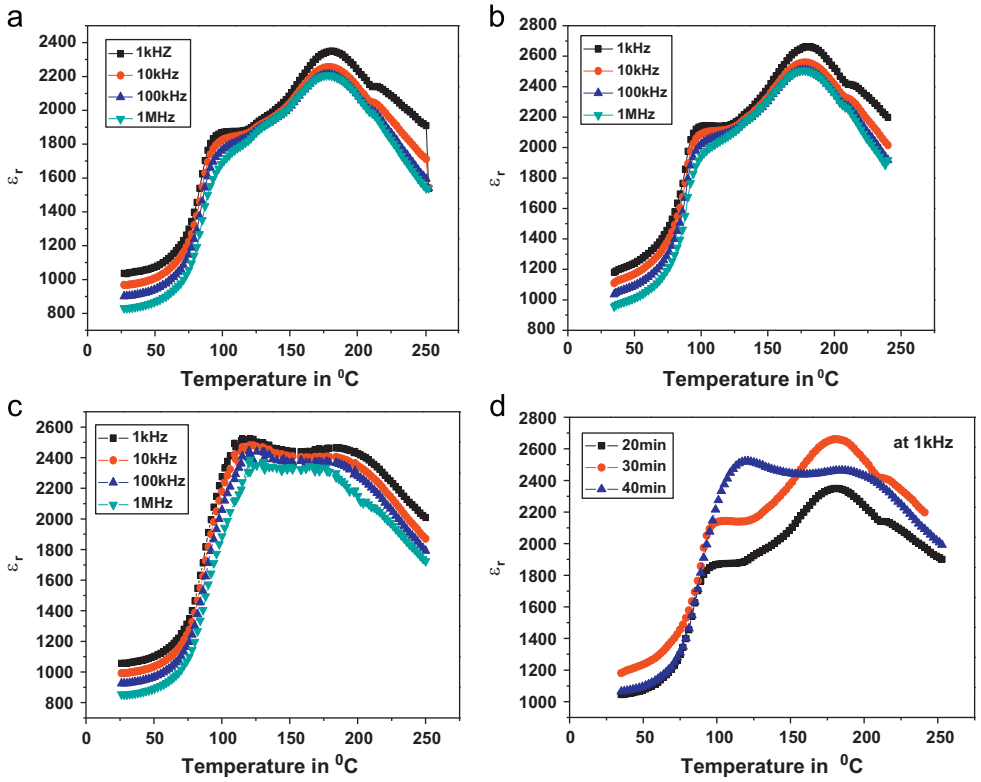

Fig. 5. Variation of ε_r with temperature at different frequencies for (a) 20, (b) 30, (c) 40 min sintered samples and (d) variation of ε_r with temperature at 1 kHz frequency for 20, 30 and 40 min sintered samples.

Fig. 5 shows the temperature dependences of ε_r at different frequencies of NBT–KNN ceramics sintered at 1150 °C for different times. From Fig. 5, it can be seen that all the sintered ceramics exhibit two dielectric anomalies near T_d and T_m/T_c temperatures. T_d is the depolarization temperatures which corresponds to the transition from a ferroelectric state to antiferroelectric state, and T_m/T_c is the temperature at which transition from an antiferroelectric state to a paraelectric state takes place. T_d and T_m are listed in Table 1. As the sintering temperature increases from 20 min to 40 min, the value of T_d increases from 97 °C to 115 °C, whereas the value of T_m increases from 177 °C to 183 °C. Increase in T_m and T_d with sintering time can be explained on the basis of porosity in the microstructure and the internal stress developed in the material. Porosity decreases the internal stress in a system and internal stress is inversely proportional to transition temperature [21]. In the present study, porosity increases with sintering time. The room temperature value of $\varepsilon_r \sim 1180$ at 1 kHz frequency is highest for the 30 min sintered NBT–KNN sample. This microwave processed the NBT–KNN system shows exceptionally high dielectric constant at room temperature as compared to conventionally processed the NBT–KNN system studied by Laoratanakul et al. [22]. This is due to high density and better microstructure obtained in the microwave processed NBT–KNN samples. This again confirms the superiority of microwave processing of samples than the conventional one.

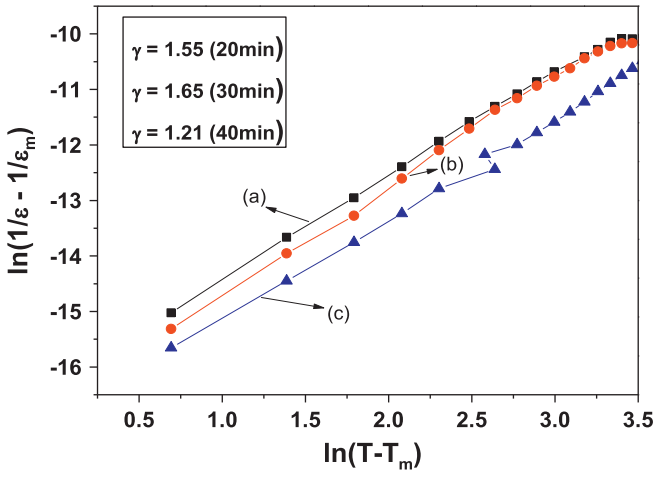

Fig. 6. Variation of $\log(1/\varepsilon_r - 1/\varepsilon_{r\ max.})$ vs. $\log(T - T_{max})$ of NBT–KNN ceramics sintered in MW furnace for (a) 20, (b) 30, and (c) 40 minutes.

As can be seen in Fig. 5, the dielectric peaks at T_m for all the ceramics are relatively broad, suggesting that the phase transitions at T_m are of diffusive in nature. In perovskite-type compounds, the diffuse phase transition occur when at least two cations occupy the same crystallographic site A or B of ABO_3 perovskite structure. A cationic disorder induced by B-site substitution is always regarded as the main cause for the appearance of diffusive behavior. However, according to previous reports, the diffusive behavior in NBT-based ceramics should attribute to a cationic disorder induced by both A-site and B-site substitutions [23]. In the solid solution of NBT–KNN ceramics, there is competition between Bi, Na and K ions to occupy A-sites, whereas there is competition between Ti and Nb ions to occupy B-sites of ABO_3 perovskite structure, which results in diffusive phase transition behavior. Diffuseness in the phase transition can be calculated by the following equation [24]:

$$(1/\varepsilon_r - 1/\varepsilon_m) = (T - T_m)^{\gamma}/C \quad (1)$$

where, ε_m is the maximum value of dielectric constant at T_m, γ is the degree of diffuseness and C is the Curie constant. γ can have a value ranging from 1 for a normal ferroelectric to 2 for an ideal relaxor ferroelectric. From the temperature vs. ε_r data at 1 kHz frequency, the graphs between $\ln(1/\varepsilon_r - 1/\varepsilon_m)$ vs. $\ln(T - T_m)$ for NBT–KNN ceramics are plotted and shown in Fig. 6. All the samples exhibit a linear relationship and by least-squared fitting the value of γ is calculated. The NBT–KNN ceramics sintered for 30 min shows a maximum value of $\gamma \sim 1.65$. This suggests that the cationic disorder is maximum in NBT–KNN samples sintered for 30 min. Fig. 7 shows the variation of dielectric constant (ε_r) and dielectric loss ($\tan\delta$) with frequency at RT of all the sintered samples. The dielectric constant decreases whereas the loss increases with the increase of frequency. The decreasing behavior of ε_r with the increase in frequency can be explained on the basis of dispersion of polarization with frequency. Dielectric polarization in a material is the sum total of the different polarization mechanisms; such as electronic,

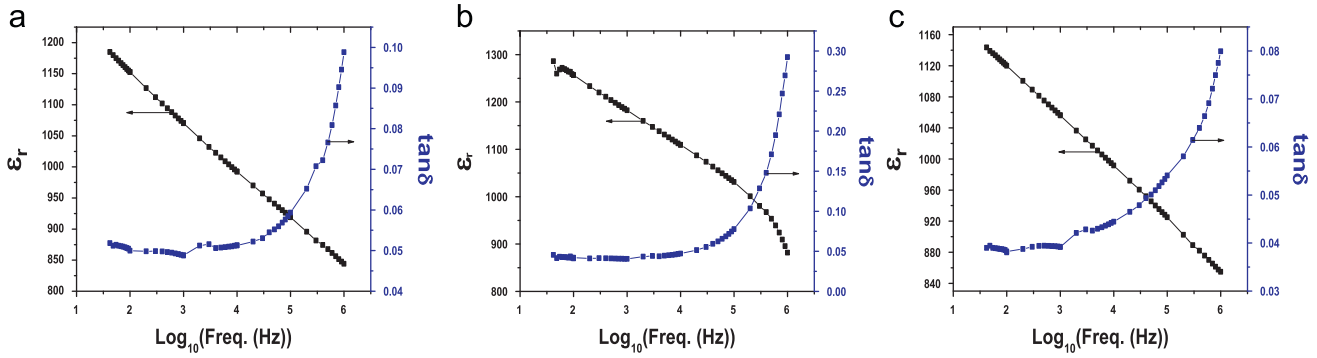

Fig. 7. Variation of ε_r and $\tan\delta$ with frequency at RT of NBT–KNN ceramics sintered at 1150 °C for (a) 20, (b) 30 and (c) 40 min.

ionic, dipolar and interfacial polarization [25]. The mechanisms of polarization have varying time response dependence on the frequency of the applied field and the net contribution of polarization to the ε_r is therefore frequency dependent. At lower frequency all the polarizations respond easily to the time varying electric field but as the frequency of the field increases different polarizations are filtered out, as a result the overall polarizations of the material decreases which leads to the decrease in the value of ε_r. The increase in dielectric loss (tan δ) with the increase of frequency occurs due to dc conductivity and dipole relaxation in NBT based systems. It is well known that, at low frequency all polarizations follow the varying ac field but an increase in frequency relaxation process occurs, which contributes to high dielectric loss in the materials [26].

In order to examine the ferroelectric nature of the microwave sintered $2P_r$ ceramics, the polarization vs. electric field (P–E) loops are measured and shown in Fig. 8. Well developed saturated loops are observed in all the samples at the room temperature. Ferroelectric parameters of the microwave sintered NBT–KNN ceramics are given in Table 2. The samples sintered for 30 min exhibit maximum values of remnant polarization ($2P_r$). The increase in $2P_r$ and decrease in E_c values of the NBT–KNN ceramics sintered for 30 min can be associated with the increase in domain wall motion and switching behavior. The highest value of $2P_r$ can be associated with the highest grain size of NBT–KNN samples sintered for 30 min. Bigger grain size results in smaller fraction of grain boundary in the material, which increases the crystalline phase

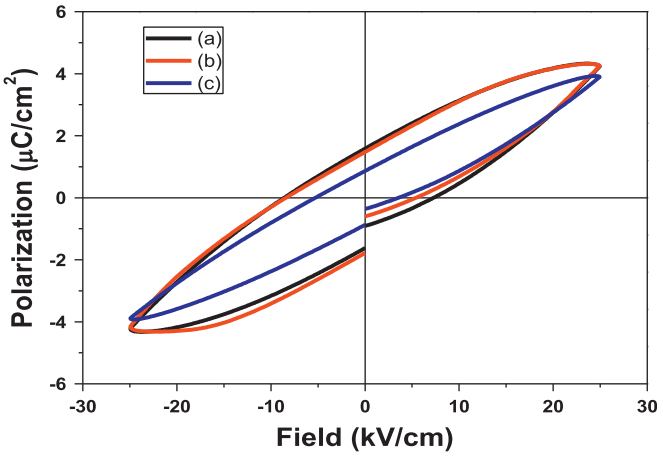

Fig. 8. P–E hysteresis loops of NBT–KNN ceramics sintered at 1150 °C for (a) 20, (b) 30 and (c) 40 min.

Table 2
Ferroelectric parameters of MW processed NBT–KNN ceramics.

Microwave sintering time (min)	$2P_r$ (μC/cm^2)	E_c (kV/cm)
20	3.2	6.2
30	3.3	5.8
40	1.74	5.6

of the whole material and consequently enhances the ferroelectric properties [26]. The value of $2P_r$ in 40 min sintered samples is decreased. This may be due to the fact that liquid phase sintering is increasing with the increase of sintering time in microwave processed NBT–KNN samples (as confirmed from SEM microstructures). As the duration of sintering time is less in microwave processed samples, increase of liquid phase sintering will decrease the density and grain growth. Also, the domain size is proportional to the grain size [27]. Therefore, the decrease of density and grain size of NBT–KNN samples, sintered for 40 min, justifies the decrease of $2P_r$ value.

4. Conclusions

Dielectric and ferroelectric properties of microwave processed NBT–KNN ceramics have been investigated in detail. Non-uniformity in grain distribution observed was attributed to incorporation of KNN into NBT lattice. Increase of phase transition temperature with sintering time is explained on the account of porosity and internal stress developed in the system. Introduction of KNN in NBT enhanced the cationic disorder, resulting in complete diffused phase transition behavior. Ferroelectric nature of the microwave processed NBT–KNN ceramics was confirmed from the P–E loops study. NBT–KNN samples sintered for 30 min showed better dielectric and ferroelectric properties.

Acknowledgments

One of the authors (Ms. Sridevi Swain) is grateful for the financial support provided by Department of Science and Technology (under INSPIRE scheme), New Delhi, India.

References

[1] G.H. Haertling, Ferroelectric ceramics: history and technology, Journal of the American Ceramic Society 82 (4) (1999) 797–818.
[2] M.D. Maeder, D. Damjanovic, N. Setter, Lead free piezoelectric materials, Journal of Electroceramics 13 (2004) 385–392.
[3] B. Jaffe, W.R. Cook, H. Jaffe, Piezoelectric Ceramics, Academic Press, London, UK, 1971, pp. 221–224.
[4] H. Nagata, M. Yoshida, Y. Makiuchi, T. Takenaka, Large piezoelectric constant and high curie temperature of lead-free piezoelectric ceramic ternary system based on bismuth sodium titanate–bismuth potassium titanate–barium titanate near the morphotropic phase boundary, Japanese Journal of Applied Physics 42 (2003) 7401–7403.
[5] G.A. Smolensky, V.A. Isupov, R.I. Agranovskaya, N.N. Kainik, New ferroelectrics of complex composition, Soviet Physics-Solid State 2 (1961) 2651–2654.
[6] B.H. Kim, S.J. Han, J.H. Kim, J.H. Lee, B.K. Ahn, Q. Xu, Electrical properties of $(1-x)(Bi_{0.5}Na_{0.5})TiO_3$–$xBaTiO_3$ synthesized by emulsion method, Ceramics International 33 (2007) 447–452.
[7] S.E. Park, K.S. Hong, Variation of structure and dielectric properties on substituting A-site cations for Sr^{2+} in $(Na_{1/2}Bi_{1/2})TiO_3$, Journal of Materials Research 12 (1997) 2152–2157.
[8] J.K. Lee, K.S. Hong, C.K. Kim, S.E. Park, Phase transitions and dielectric properties in A-site ion substituted $(Na_{1/2}Bi_{1/2})TiO_3$ ceramics (A=Pb and Sr), Journal of Applied Physics 91 (2002) 4538.
[9] M. Raghavender, G.S. Kumar, G. Prasad, A-site substitution-controlled dielectric dispersion in lead-free sodium bismuth titanate, Pramana—Journal of Physics 72 (2009) 999.

[10] D. Lin, K.W. Kwok, H.L.W. Chan, Structure and electrical properties of $(Bi_{0.5}Na_{0.5})_{1-x-y-z}$ $Ba_xSr_yCa_zTiO_3$ lead-free piezoelectric ceramics, Journal of Physics D: Applied Physics 40 (2007) 5344.

[11] K. Yoshii, Y. Hiruma, H. Nagata, T. Takenaka, Electrical Properties and depolarization temperature of $(Bi_{1/2}Na_{1/2})TiO_3$–$(Bi_{1/2}K_{1/2})TiO_3$ lead-free piezoelectric ceramics, Japanese Journal of Applied Physics 45 (5B) (2006) 4493–4496.

[12] S. Zhao, G. Li, A. Ding, T. Wang, Q. Rui, Ferroelectric and piezoelectric properties of $(Na, K)_{0.5}Bi_{0.5}TiO_3$ lead free ceramics, Journal of Physics D: Applied Physics 39 (2006) 2277.

[13] A.B. Kounga, S.T. Zhang, W. Jo, T. Granzow, J. Rodel, Morphotropic phase boundary in $(1-x)Bi_{0.5}Na_{0.5}TiO_3$–$xK_{0.5}Na_{0.5}NbO_3$ lead-free piezoceramics, Applied Physics Letters 92 (2008) 222902–222903.

[14] Q. Zhang, Y. Zhang, F. Wang, Y. Wang, D. Lin, X. Zhao, H. Luo, W. Ge, D. Viehland, Enhanced piezoelectric and ferroelectric properties in Mn-doped $Na_{0.5}Bi_{0.5}TiO_3$–$BaTiO_3$ single crystals, Applied Physics Letters 95 (2009) 102904.

[15] V.A. Isupov, Ferroelectric $Na_{0.5}Bi_{0.5}TiO_3$ and $K_{0.5}Bi_{0.5}TiO_3$ perovskites and their solid solutions, Ferroelectrics 315 (2005) 123–147.

[16] E. Wu, PowdMult. An, Interactive X-ray powder diffraction data interpretation and indexing program, Version 2 (1978) 2.

[17] M. Matsubara, T. Yamaguchi, K. Kikuta, S. Hirano, Sinterability and piezoelectric properties of $(K,Na)NbO_3$ ceramics with novel sintering aid, Japanese Journal of Applied physics 43 (2004) 7159–7163.

[18] A. Mondal, A. Shukla, A. Upadhyaya, D. Agrawal, Effect of porosity and particle size on microwave heating of copper, Science of Sintering 42 (2010) 169–182.

[19] M.V. Ramana, S.R. Kiran, N.R. Reddy, K.V.S. Kumar, V.R.K. Murthy, B.S. Murty, Synthesis of lead free sodium bismuth titanate (NBT) ceramic by conventional and microwave sintering methods, Journal of Advance Dielectrics 1 (1) (2011) 71–77.

[20] B. Malic, J. Bernard, J. Holc, D. Jenko, M. Kosec, Alkaline-earth doping in $(K,Na)NbO_3$ based piezoceramics, Journal of the European Ceramic Society 25 (2005) 2707–2711.

[21] T.T.K. Hiroshima, T. Kimuru, Effects of microstructure and composition on the Curie temperature of lead barium niobate solid solutions, Journal of the American Ceramic Society 79 (1996) 3235–3242.

[22] P. Laoratanakul, R. Yimnirun, S. Wongsaenmai, Phase formation and dielectric properties of bismuth sodium titanate potassium sodium niobate ceramics, Current Applied Physics 11 (2011) S161–S166.

[23] Y. Guo, K. Kakimoto, H. Ohsato, Ferroelectric-relaxor behavior of $(Na_{0.5}K_{0.5})NbO_3$-based ceramics, Journal of Physics and Chemistry of Solids 65 (2004) 1831–1835.

[24] C. Karthik, N. Ravishankar, M. Maglione, R. Vondermuhll, J. Etourneau, K.B.R. Varma, Relaxor behavior of $K_{0.5}La_{0.5}Bi_2Ta_2O_9$ ceramics, Solid state communications 139 (2006) 268–272.

[25] A.K. Singh, T.C. Goel, R.G. Mendiratta, O.P. Thakur, C. Prakash, Dielectric properties of Mn-substituted Ni–Zn ferrites, Journal of Applied Physics 91 (2002) 6626.

[26] P. Palei, P. Kumar, D.K. Agrawal, structural and electrical properties of microwave processed Ag modified KNN-LS ceramics, Journal of Microwave Power and Electromagnetic Energy 46 (2) (2012) 76–82.

[27] W. Cao, C.A. Randall, Grain size and domain size relations in bulk ceramic ferroelectric materials, Journal of Physics and Chemistry of Solids 57 (10) (1996) 1499–1505.